LAND COVER AND WATER TYPE CLASSIFICATION USING IMAGES CAPTURED BY THE PHLIPPINES' FIRST EARTH-OBSERVING MICROSATELLITE DIWATA-1

Jasper Madalipay, Gay Jane Perez, Louisse Anne Fulgencio, Mark Jayson Felix, Marco Macapagal, Ellen Mae Leonardo, Francisco Miguel Felicio, Kaye Vergel and Shielo Namuco
Remote Sensing Product Development Project, PHL-Microsat Program, Institute of Environmental Science and Meteorology, University of the Philippines Diliman
Email: jtmadalipay@up.edu.ph, gpperez1@up.edu.ph, lcfulgencio@up.edu.ph, mark_jayson.felix@upd.edu.ph, mdmacapagal@up.edu.ph, ecleonardo@up.edu.ph, micofelicio@gmail.com, kookaye@gmail.com, sbnamuco@up.edu.ph

KEYWORDS: supervised classification, confusion matrix, producer's accuracy, user's accuracy, NDVI

ABSTRACT: Diwata-1 is the Philippines' first earth-observing microsatellite with multispectral and high-resolution telescopes intended for a wide spectrum of applications including agriculture, forestry, urban, and coastal studies. In this study, land cover and water type classification was performed using Diwata-1 images captured across the country. Supervised classification using maximum likelihood method was utilized to categorize different land cover and water types. The accuracy of the generated land and water classification maps were evaluated using error matrices based on high-resolution images from Google Earth. Based on the results, shallow water pixels were successfully delineated from the deep waters. Vegetated areas were differentiated from non-vegetated ones; however, several bare and built-up pixels were misclassified mainly due to resemblances in spectral information. Nonetheless, average overall accuracy of 79.46% and average kappa coefficient of 0.6279 indicated good accuracy for the classified images. These preliminary results may pave the way for a more detailed classification such as identification of different vegetation types. Furthermore, land cover and water type classification maps can aid decision makers in assessment, planning and management of the Philippines' environmental resources.

1. INTRODUCTION

The Philippines' first microsatellite, Diwata-1, was successfully deployed into orbit from the International Space Station in April 27, 2016 for earth observation purposes. The 50-kg microsatellite with dimension of 55 x 35 x 55 centimeters is a low earth orbit (LEO) satellite with an estimated altitude of 400 kilometers. Diwata-1 has four payloads: the high precision telescope (HPT), spaceborne multispectral imager (SMI) with liquid crystal tunable filter (LCTF), wide field camera (WFC) and the middle field camera (MFC). The HPT has four CCDs each in the red, green, blue and near-infrared region. It has a ground sampling distance (GSD) of 3 m and a field of view of 1.9 x 1.4 km at an altitude of 400 km. The SMI with LCTF has two CCDs, one for each visible (433 – 740 nm) and near-infrared (730-1020 nm) regions. It has a GSD of 66 meters and a field of view of 32 x 43 km. WFC is a simple camera with a panchromatic CCD with a field of view of 180o x 134o and GSD of 7 km. Lastly, MFC is an engineering payload with a colored CCD, capable of capturing images at 185 m resolution and field of view of 121.9 x 91.4 km.

The SMI and the HPT are the Diwata-1 payloads that are used primarily for scientific applications. The high spatial resolution of the HPT is useful in determining the extent of damages from disasters. The SMI with LCTF having bands ranging from 433 and 1020 nm at one nanometer interval is vital in the assessment of vegetation condition. Various vegetation indices such as the normalized difference vegetation index (NDVI) and the green normalized vegetation index (GNDVI) can be obtained using the bands of the SMI. In addition, land cover classification maps can be derived using the SMI and the HPT images.

Using the HPT and SMI images captured by the Diwata-1 microsatellite, this study aims to generate land cover and water type classifications for various areas in the Philippines. In addition, this study intends to demonstrate the use of these classification maps as aids in the assessment of damages due to disasters.

2. METHODOLOGY

2.1 Datasets and study area

The primary data in this study are the images captured by the HPT and SMI payloads of Diwata-1. For the land cover and water type classification using the HPT images, two different sites were studied: the agricultural area of Asuncion in the province of Davao del Norte (Figure 1a) and the flooded part of Enrile in the province of Cagayan (Figure 1b). The scene in Asuncion (7.523010° N, 125.762160° E) was captured on August 17, 2016 and located in

the southern part of the Philippines where bananas are commonly cultivated. The scene in Enrile (17.559090°, 121.739090°) in the northern part of the country was taken on October 24, 2017, five days after the Super Typhoon Lawin (international name: Haima) hit the northern portion of the Luzon island.

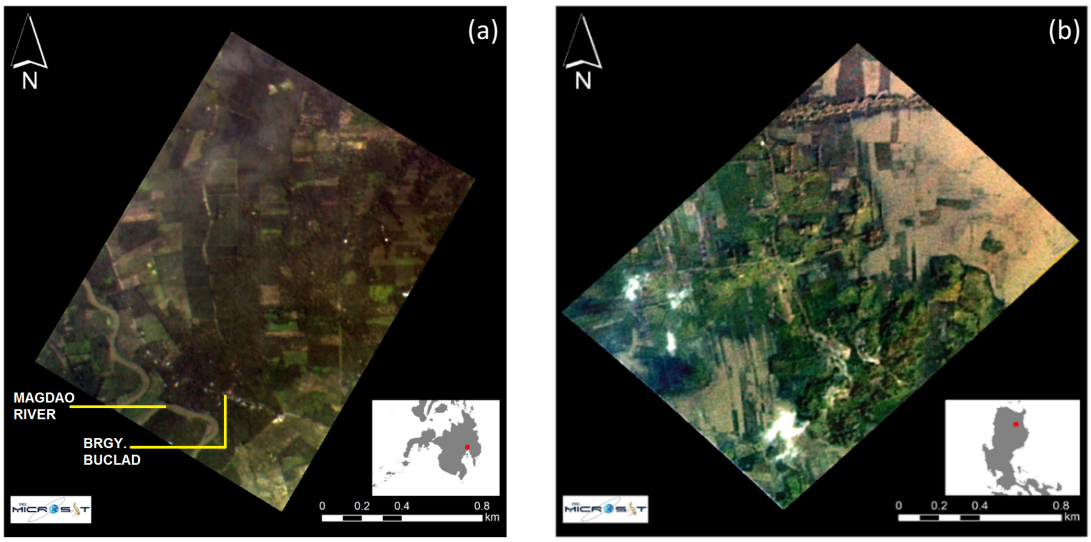

Figure 1. True-color composite of the HPT images in (a) Asuncion, Davao del Norte and (b) Enrile, Cagayan for land cover classification.

For the land cover and water type classification using SMI images, two scenes were studied: coastal portion of the Albay province (Figure 2a) and the central part of Ilocos Norte (Figure 2b). The scene in Albay province (13.316200°, 123.844560°) is in the eastern seaboard of the southern tip of Luzon and captured on April 24, 2017. The image of Ilocos Norte (18.140200°, 120.657830°), captured on April 5, 2017, is situated in the northwestern part of Luzon and facing the Western Philippine Sea.

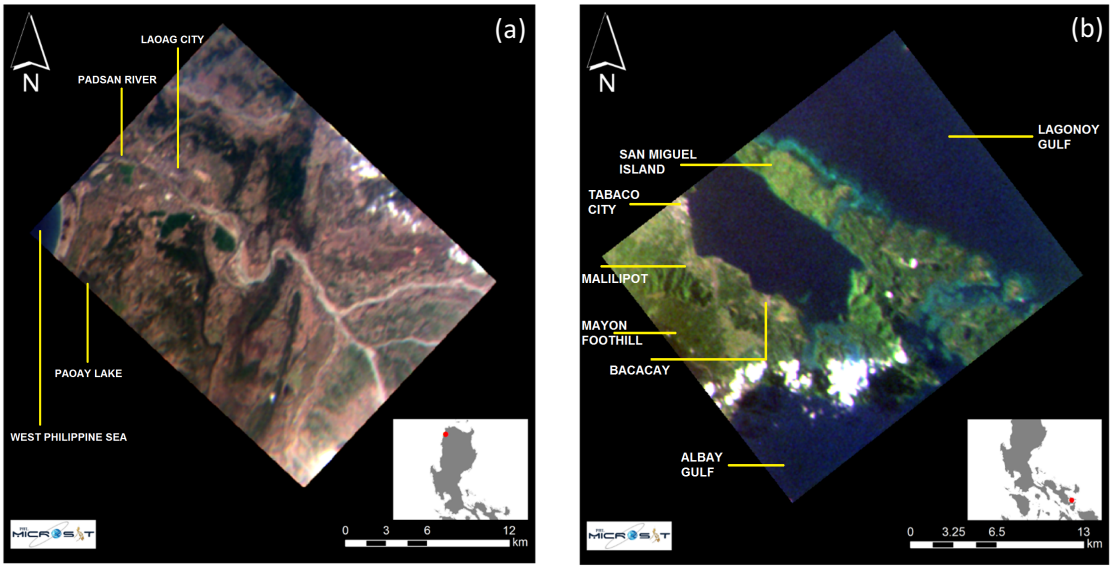

Figure 2. True-color composite of the SMI images in (a) Ilocos Norte and (b) Albay for land cover classification.

The post-disaster image of Enrile, Cagayan captured by the HPT sensor was compared with a Landsat-8 image taken on October 26, 2016, two days after the acquisition of the Diwata-1 image, to evaluate the capability of the HPT in disaster assessment. A land cover classification map was derived from the Landsat image and compared to the Diwata-1 classification map to assess the damage in the area due to the typhoon.

2.2 Radiometric calibration and georeferencing

All raw satellite images undergo preliminary steps before higher level remote sensing products can be derived. In studying the land cover and water types in several areas in the Philippines using Diwata-1, several preprocessing were done. The flowchart of the derivation of classification maps from raw images is shown in Figure 3.

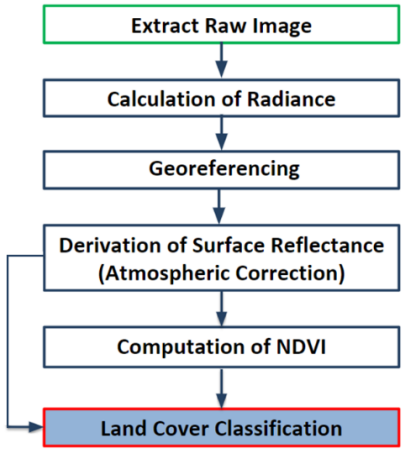

Figure 3. Flowchart of land cover classification using Diwata-1.

The first step in the classification of Diwata-1 images is the extraction of an image from the binary data. The captured raw images were saved in digital numbers (DN). These raw images were converted to radiance using the calibration parameters derived from the pre-launch radiometric tests. The calibration coefficient is given by Equation 1,

$$C(\lambda) = \frac{t_{exp}\, L(\lambda)_{is}}{(DN - dark\ count)} \qquad \frac{\mu W \cdot s}{m^2 \cdot nm \cdot sr} \tag{1}$$

where, t_{exp} is the exposure time used in the radiometric calibration experiment, $L(\lambda)_{is}$ is the radiance at the integrating sphere at certain wavelength and ***DN*** is the DN value of the images 10 bit format. ***Dark count*** is the mean value of CCD's optical black region. The calibration coefficient is dependent on the wavelength and the gain. Finally, the radiance of an image was calculated using Equation 2,

$$L(\lambda) = \frac{C(\lambda) \cdot (DN - dark\ count)}{t_{act\ exp}} \qquad \frac{\mu W}{m^2 \cdot nm \cdot sr} \tag{2}$$

where $C(\lambda)$ is the calibration coefficient with the given acquisition gain and $t_{act\ exp}$ is the exposure time used in the actual image acquisition.

After the radiance values were obtained, every pixel of an image was assigned with geographic coordinates. The exact location was determined by overlaying an image accurately in Google Earth. The geographic coordinates of the center and corner pixels of each images were used as input in *image to map registration* tool in the ENVI software. Furthermore, several random tiepoints inside the bounds of the image were added to obtain a more accurate georeferenced image especially in areas of uneven elevation. The individual georeferenced bands were stacked afterwards to obtain composite bands.

The georeferenced image with radiance values were subsequently converted to top-of-atmosphere (TOA) reflectance, which was used as input for the atmospheric correction of all Diwata-1 images. TOA reflectance is given by equation 4,

$$\rho_{TOA}(\lambda) = \frac{L(\lambda) \cdot \pi \cdot d_o^2}{ESUN(\lambda) \cdot cos\theta} \tag{3}$$

where $L(\lambda)$ is the radiance at certain wavelength, do is the sun-earth correction factor, $ESUN(\lambda)$ is the extraterrestrial solar irradiance as a function of wavelength and θ is the sun zenith angle.

2.3 Atmospheric correction using QUAC

In remote sensing, it is important to apply atmospheric correction to remove atmospheric effects and obtain correct reflectance on ground level. In this study, the quick atmospheric correction (QUAC) method integrated in the ENVI software was used. The QUAC method is a fast and approximate atmospheric correction technique used for multi- and hyperspectral images with bands in the visible to near-shortwave infrared region. It is an in-scene approach that only requires approximate specification of the center wavelengths of the bands and their radiometric calibration. Because additional metadata and radiation transport calculations are not involved in the method, the process is significantly faster (Bernstein et al., 2012).

Cloud masking was first done for the atmospheric correction method to work accurately. Using the threshold method, all the bright cloud and dark cloud shadow pixels were removed. The cloud masked images in TOA reflectance were used as input in QUAC. Since the sensors of Diwata-1 are not in the list of sensor types in ENVI, the generic sensor type was utilized in the process. QUAC identifies a sufficiently close surrogate sensor for the process based on the number and location of the wavelength bands in the image when the generic sensor type is selected (Bernstein et al., 2012). After the QUAC process, a scale factor was applied to obtain a surface reflectance ranging from 0 to 1.

2.4 Computation of NDVI

The derivation of surface reflectance from satellite sensors leads to numerous remote sensing applications. One of which is the derivation of vegetation indices such as the normalized difference vegetation index (NDVI). It uses the red and near-infrared bands to measure vegetation condition (Rouse et al., 1974). The index is widely used to assess the patterns and modification in land cover through time by investigating the changes in the values of this index in an area (Morawitz et al., 2006). In addition, the NDVI is also used for classification of various land cover classes such as grassland, woodland, forest, cultivated crops and bare ground (Defries et al., 1994). In this study, the ability of the NDVI to classify different land cover types was utilized to improve the classification of SMI images.

2.5 Image classification

For the classification of land covers and water types, the supervised classification using the maximum likelihood method in ENVI was used. The supervised classification technique is commonly used for the quantitative analysis of remote sensing image data. In this study, the most common supervised classification method was employed – the maximum likelihood algorithm. The maximum likelihood method needs sufficient training data to estimate a probability distribution for a cover type and have a more accurate classification (Richards and Jia, 2006). Several training data were selected and the class of each was determined using the Google Earth software. For the land covers, the classes were categorized to bare land, built-up and vegetation. The vegetation class is defined as any land area that is covered by vegetation such as grasslands, shrublands and forests. Bare land is categorized as land type wherein the soil is exposed. Bare land includes vacant agricultural plots, dried tributaries of water bodies (e.g. rivers) and denuded forests. Built-up class is any constructed artificial landscape (e.g. buildings and roads). Meanwhile, the water types were classified to turbid/shallow water and clear water. For the clear water category, it is the deep dark-bluish water wherein there is no effect of bottom reflectance and suspended matter (e.g. deep ocean waters). Lastly, the turbid/shallow water class is affected by suspended matter and bottom reflectance and can be greenish or brownish in color. Turbid/shallow waters include rivers, watered agricultural areas and ponds.

2.6 Accuracy Assessment

To validate the result of the classification maps, accuracy assessment was done in all images. A total of 101 random points per classification map were selected as validation points using the stratified random sampling since the classes have unequal sizes. The class of every random point was validated using Google Earth. An error or confusion matrix, which includes the producer's and user's accuracy, was used to evaluate the accuracy of the derived classification maps. The producer's accuracy was obtained by dividing the total number of correct pixels in a category by the total number of pixels of that category as derived from the reference data (Congalton, 1991). On the other hand, the user's accuracy was calculated by dividing the total number of correct pixels in a category by the total number of pixels that were classified in that category. The user's accuracy indicates the probability that a pixel classified on the map or image represents that category on the ground (Story and Congalton, 1986). Finally, the kappa coefficient was obtained for each classification to determine the strength of agreement of the classification map and the reference map, Google Earth. The kappa coefficient was computed using equation 4

$$\kappa = \frac{\pi_0 - \pi_e}{1 - \pi_e} \quad (4)$$

where π_o is the observational probability of agreement and π_e is the hypothetical expected probability of agreement. The strength of agreement based from the kappa coefficient were categorized to poor (<0.00), slight (0.00-0.20), fair (0.21-0.40), moderate (0.41-0.60), substantial (0.61-0.80) and almost perfect (0.81-1.00) (Landis and Koch, 1997).

3. RESULTS AND DISCUSSION

3.1 Land Cover Classification Maps

The result of the land cover classification of HPT images in (a) Asuncion, Davao del Norte and (b) Enrile, Cagayan is shown in Figure 4. The 3-meter resolution image of Asuncion (Figure 4a) is composed of vegetation, bare soil, turbid/shallow water and built-up classes with a total area of is 2,797,290 m^2. The major land cover is vegetation covering 1,899,324 m^2 or 67.9% of the total area. The grasslands, banana and coconut plantations, agricultural and forest areas were successfully classified as vegetation. Bare land covers a total of 771,399 m^2 which constitutes 27.57% of the total scene. The bare land class is composed primarily of uncultivated agricultural lands. The turbid water class, which includes the Magdao River and some watered agricultural plots, comprises 3.96% of the total area and equivalent to 110,808 m^2. Lastly, the smallest chunk in the classification map is the built-up class covering 0.56% or 15,759 m^2 of the total scene and composed of houses in Brgy. Buclad.

The HPT image in Enrile, Cagayan (Figure 4b) with a total area of 3,012,926 m^2 has the same classes as the Asuncion scene. Vegetation covered the largest space with an area of 1,644,271 m^2, about 54.57% of the scene. Vegetation is composed of agricultural crops, grassland and dense trees. The turbid/shallow water has an area of 1,004,667 m^2 or 33.35% of the land cover map. Based from previous Google Earth images, the shallow/turbid water are flooded agricultural lands due to typhoon rains brought by Lawin. Bare soil constitutes to 12.07% of the total area or 363,719 m^2. The land cover with the smallest percentage is built-up, covering merely 269 m^2 or 0.009% of the total scene.

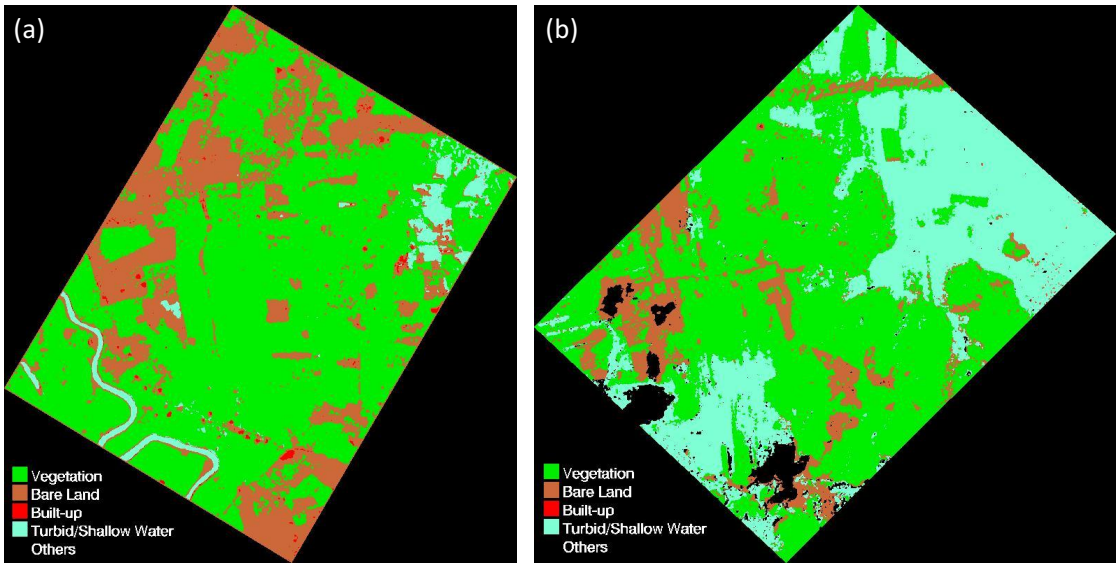

Figure 4. Land cover classification maps of (a) Asuncion, Davao del Norte and (b) Enrile, Cagayan from Diwata-1's HPT.

For the SMI images, the land and water classification maps of Ilocos Norte and Albay derived using supervised classification is shown in Figure 5. The 60-meter resolution image captured in Ilocos Norte (Figure 5a) has a total land area of 566.9 km^2. Majority of the scene is covered by bare soil covering an area of 363.38 km^2 or 64.1% of the total scene. Uncultivated agricultural lands, barren soil, floodplains along the river and beaches are included in the bare land class. Vegetation is the second largest class in the map with an area of 153.18 km^2 or 27.02% of the captured scene. The vegetation class in the scene is composed primarily of agricultural crops and forests. The built-up class, which includes the urban area of Laoag City and other municipalities in the province, covered 6.46% of the total area or 36.5 km^2. Paoay Lake, Padsan River and the shallow portion of the West Philippine Sea were successfully classified as turbid/shallow water. The turbid/shallow water type has an area of 10.49 km^2, about

1.85% of the classification map. The deep portion of the West Philippine Sea was successfully classified as clear water and has an area of 3.21 km^2 that is equivalent to 0.57% of the total scene.

The derived land cover and water type classification map of Albay (Figure 5b) has a total area of 627.32 km^2. Similar to the derived map of Ilocos Norte, the supervised classification method successfully categorized the image to five land and water classes previously mentioned. The largest class in the map is clear water with an area of 315.29 km^2 and makes up 50.26% of the scene. The deep portions of Albay and Lagonoy Gulfs were successfully classified as clear water. The vegetation class, which includes the lush vegetation in Bacacay area and on the foothills of Albay, has an area of 178.93 km^2 or 28.52% of the classification map. Turbid/shallow water class covered an area of 75.29 km^2 or 12.00% of the scene and includes the shallow waters and fringing reefs in the municipality of Bacacay. Bare land makes up 8.70% of the scene or about 54.57 km^2. The uncultivated agricultural areas on the foothills of Mayon Volcano in the municipalities of Malilipot and Santo Domingo and in the island of San Miguel in Bacacay were successfully categorized as bare land. Lastly, the built-up class only covered an area of 3.24 km2 or 0.52% including the residences in the central barangays of Tabaco City and Bacacay.

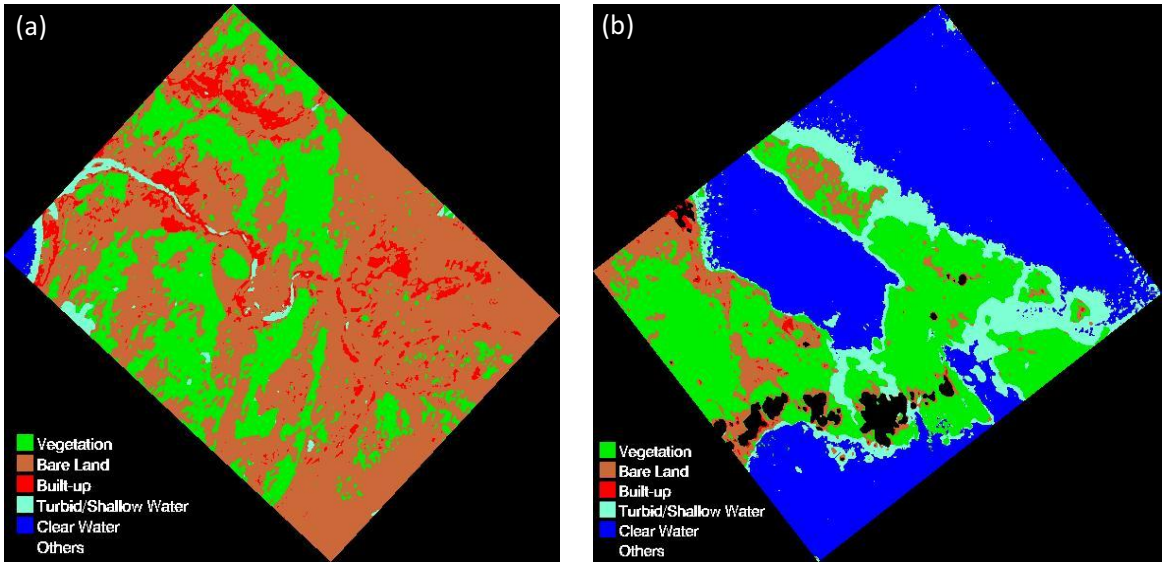

Figure 5. Land cover classification maps of (a) Ilocos Norte and (b) Albay from Diwata-1's SMI.

3.2 Accuracy assessment of classification maps

The derived classification map of Asuncion, Davao del Norte (Figure 4a) acquired by the HPT sensor yielded a high overall accuracy of 86.14% where 87 points were correctly classified out of the 101 validation points. The computed producer's accuracy, which indicates the probability of a reference pixel being correctly classified, is generally high since all the classes have greater than 80% accuracy. The turbid/shallow water class has a perfect 100% producer's accuracy which means that the turbid or shallow waters on the grounds of Asuncion can be easily classified. The same is also true for vegetation and bare land classes which yielded high producer's accuracy of 87.67% and 80.00%, respectively. The user's accuracy in the Asuncion image is highest for the vegetation class with 94.12%. This means that there is a high chance that the vegetation in the derived classification map is really vegetation on the ground. In addition, the turbid/shallow water and bare land classes have also relatively high user accuracy of 75.00% and 71.43%, respectively. The 0.00% user's accuracy for the built-up class means that the artificial surfaces on the classification maps are different classes on the ground. However, this is not always true since there is only one validation point for urban/built-up due to its smaller size relative to other classes. The user's accuracy for built-up can be improved by adding more random validation points for that class.

The Asuncion image has a kappa coefficient of 0.69 indicating a substantial level of agreement between the derived classification map and Google Earth. The primary source of error in the misclassification of some pixels is the small shift in the geographic location of the classification map compared to Google Earth. The small discrepancy in georeferencing in some portions of the image and the several points from the stratified random sampling located near class boundaries contributed to about 8% of error in the overall accuracy of the classification. Moreover, the gap in the acquisition dates of the reference data and the classification map is also factor since the available cloudless Google Earth images used for validation were eight and 12 months prior the acquisition date of the HPT image. The vegetation and bare land covers may be affected by this gap. Agricultural lands wherein the crops were

already harvested during Diwata-1 acquisition were classified as bare land but it may be vegetated in the reference image since the capture date was different.

The post-disaster classification map of Enrile, Cagayan (Figure 4b) has a substantial overall accuracy of 72.28% based from the result of the confusion matrix. Similar to the HPT image in Asuncion, the derived classification map of Enrile yielded a high producer's accuracy of 84.62% and 77.59% for the turbid/shallow water and vegetation class, respectively. However, the bare land class has a low producer's accuracy of 35.29%. Bare land areas in Enrile were often misclassified as vegetation. On the other hand, the user's accuracy is highest for vegetation with 81.82%, while the turbid/shallow water class has a substantial 64.71% user's accuracy. The user's accuracy is lowest for bare land with 50.00%, indicating that there is a moderate chance that the bare land is different on the ground, for this case turbid/shallow water or vegetation.

From the result of the user's and producer's accuracy, the classification image of Enrile has a kappa coefficient of 0.5225, signifying a moderate level of agreement with the reference data. For this case, the main cause of error is the misclassification of bare soil, wherein 59% was categorized as vegetation. Again, the issue of georeferencing is one of the factors why some pixels were incorrectly categorized. In addition, the time of acquisition of the image is a significant factor in the misclassification of bare land areas. Since the image was captured early in the morning (07:29am local time), the spectral response of surfaces is slightly different compared when the image acquisition is done at optimal time. Moreover, since the Diwata-1 image was taken three days before the Google Earth image, there were already significant changes particularly in the flooded regions. About 32% of the turbid/shallow water in the classification map were already vegetation when validated using the reference image. This means that several flooded agricultural lands as seen by Diwata-1 already dried up after two days since some previously soaked agricultural crops were already visible from the reference data.

The generated classification map of Ilocos Norte (Figure 5a) acquired by the SMI has an overall accuracy of 72.28%, where 73 out of the 101 random points were correctly classified. The clear water has a perfect producer's accuracy of 100%, however, there is only one random point for this class. In addition, the bare land class also yielded a high producer's accuracy of 83.93%, wherein 47 random points on the ground were actually classified as bare land. The built-up and turbid/shallow water classes both have low producer's accuracy of 25.00%. The built-up structures on the ground were usually classified as bare soil. For the user's accuracy, the clear water class has a perfect accuracy of 100% but this is because there is only one validation point for this class. Vegetation and bare land yielded a relatively high user's accuracy of 85.19% and 73.44%, respectively. The turbid/shallow water class has a moderate user's accuracy of 50.00%, however, there are only two random points for this class. The user's accuracy is lowest for the built-up class wherein only 14.29% were correctly categorized. Most of the classified urban structures in the derived land cover map were bare land on the group.

Among the four classification maps derived from Diwata-1 images, the scene in Ilocos Norte has the lowest kappa coefficient (0.4957). However, the classification map still has a moderate level of agreement with the reference data. The low user's and producer's accuracy of the built-up class have significant contribution to the relatively low kappa coefficient. Most built-up pixels from the classification map are bare land on the ground. In opposite, most built-up areas on the ground were classified as bare land. Since built-up structures and bare areas have similarities in spectral response in the optical region, these two classes are often misclassified. Another source of error in misclassification is the mixing of several surfaces in a single pixel. There are some regions in the image where some patches of trees are situated in elevated barren areas. Since SMI has a coarser resolution of 60 meters compared to HPT (3 meters), the issue of mixed pixels is more evident, hence some bare land regions were classified as vegetation and vice-versa. This is also true for bare land and built-up classes as residences usually have bare soils in the vicinity, especially for Ilocos Norte since it is a provincial area. Similar to the HPT images, a small error in georeferencing is also a cause of misclassification of some pixels and this issue is more apparent for the SMI images since the land features include hills and mountains. The uneven elevation of the scene due to these features means more distorted pixels, particularly affecting the hilly areas where there is mixing of bare soil and vegetation.

The SMI classification map of Albay (Figure 5b) has a higher overall accuracy of 87.13% than the SMI map of Ilocos Norte. The producer's accuracy is very high for clear water (98.00%) indicating that the clear water on the ground can be easily classified. Producer's accuracy is also relatively high for vegetation and bare land classes, with 88.46% and 83.33% accuracy, respectively. The turbid/shallow water class has a moderate accuracy of 61.11% and there is a slight chance that the turbid water can be categorized as vegetation in the classification map. The built-up class has 0.00% producer's accuracy but this is due to the lone misclassified random point. On the other hand, the user's accuracy is very high for clear and turbid/shallow water with 98.00% and 91.67% accuracy, respectively. Moreover, vegetation also has high user's accuracy of 79.31%. The classification map has a moderate user's accuracy of 55.56% for bare land and has a small chance that a certain bare land class is actually vegetation

on the ground. Similar to Asuncion classification map, the user's accuracy for built-up is 0.00%, but again this is due to the lone validation point for that class.

The kappa coefficient for the Albay classification map is 0.8033, which means that it has a substantial (close to almost perfect) agreement with the Google Earth data. The Albay map has the highest overall accuracy and kappa coefficient among the four classification maps obtained from Diwata-1. The error in classification is minimal since both user's and producer's accuracy are relatively high. One of the causes of the inaccuracy is the misclassification of turbid/shallow water as vegetation. Since the fringing reefs near the coast have similarities with vegetation class in the visible spectrum, about 55% percent of the turbid/shallow water on the ground were classified as vegetation. Similar to the result of the Enrile classification map, some vegetated areas were misclassified as bare soil since the acquisition of the image was outside the optimal time. The image was taken at 04:39pm local time, hence the spectral response of the surface changed slightly.

The summary of the user's accuracy of the studied land cover and water type classes across four locations is shown in Figure 6. The clear water class has the highest user's accuracy, with an average accuracy of 99%. This high accuracy is due to the inclusion of the NDVI for better classification of vegetation and water bodies. While other classes like vegetation and bare soil have positive or close to zero NDVI values, clear water have negative values since it reflects more in the visible band than it does in the near-infrared region (Al-doski et al., 2013). For both the HPT and SMI images, the user's accuracy for vegetation class is generally high with an average accuracy of 85.11%. Again, the NDVI calculation for the two SMI images helped in better classification of the vegetation class. In addition, the broad red band of the HPT sensor centered at 684 nm extends from 658 nm to 825 nm, hence signals are also detected in the near-infrared region. Because of this, vegetated areas in the HPT images were also easily classified. The 70.35% average user's accuracy for the turbid/shallow water class still shows strong agreement with the reference data. For bare land, the average user's accuracy across the four sites is 62.61%. The effect of the acquisition time is apparent for the Enrile and Albay classification maps, since they are outside the optimal acquisition window. The low user's accuracy and misclassification of built-up areas is mainly due to the similarities in their spectral response with bare soil, their size and sparsity in the scene and the number of validation points for the class.

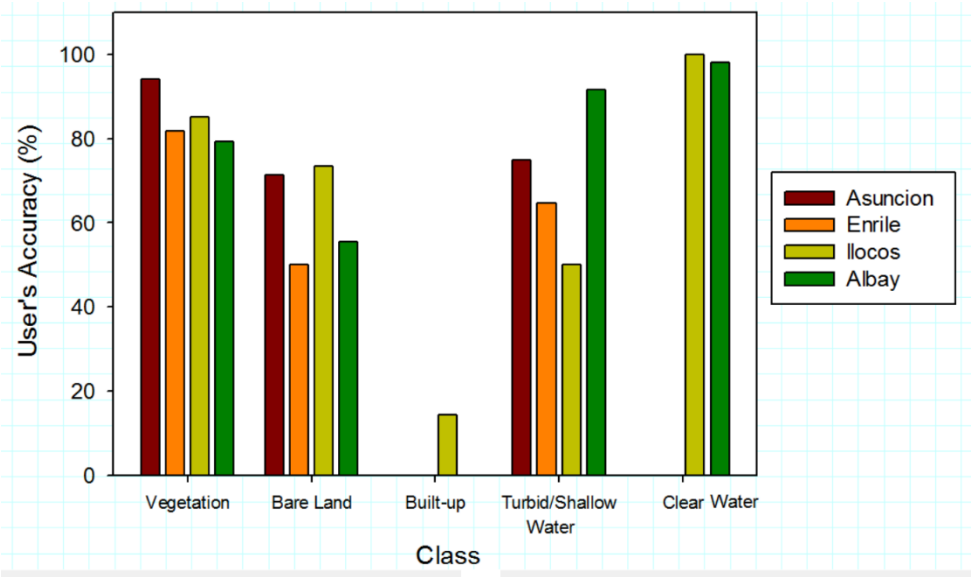

Figure 6. User's accuracy of the derived classification maps from Diwata-1.

The producer's accuracy of the of the land cover and water types across the four study sites is summarized in Figure 7. The producer's accuracy is highest for clear water with average accuracy of 99%, equal to the obtained user's accuracy value. Vegetation has a high average producer's accuracy of 79.40% in those four sites signifying that the vegetation on the ground can be easily classified using the Diwata-1 images. Bare soil areas in all study sites still have strong agreement with the result of the classification maps since the average producer's accuracy is 70.64%. The producer's accuracy for the turbid/shallow water class is high for HPT images, however, it is relatively low for SMI images especially for the Ilocos scene. The built-up class has also the least producer's accuracy since it has the smaller area and the least number of validation points, making it challenging to assess.

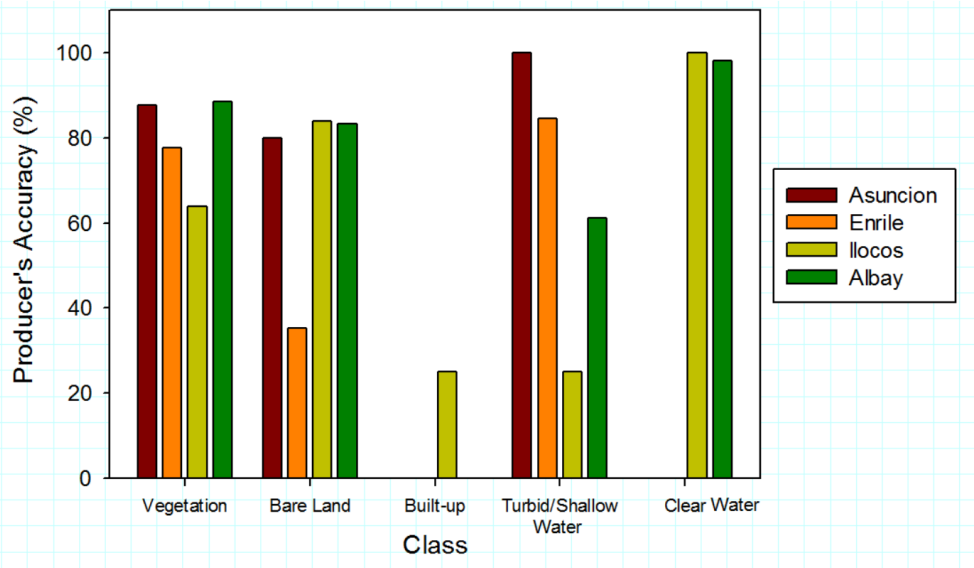

Figure 7. Producer's accuracy of the derived classification maps from Diwata-1.

The overall accuracy and kappa coefficients of the four classification maps from Diwata-1 are summarized in Table one. The classification map of Albay has the strongest agreement with the reference data since both the overall accuracy and kappa coefficient are high. For the classification map of Ilocos Norte, the overall accuracy is still high, however, the kappa coefficient is only moderate and it is the lowest among the four maps. The low kappa coefficient is due to the challenge of classifying built-up and bare soil in the scene, especially since majority of the area is covered with bare soil, and the mixing of features in pixels. In addition, the kappa coefficient is generally affected by the difference in the acquisition dates of the reference image and the Diwata-1 images. Nonetheless, looking at the overall performance of Diwata-1 in land cover and water type classification, the high average overall accuracy of 79.46% and average kappa coefficient of 0.6279 means that the Philippine microsatellite is capable of generating good accuracy classification maps that can be used for various applications.

Table 1. Overall accuracy and kappa coefficient of the Diwata-1 classification maps.

Sensor	Location	Overall Accuracy (%)	Kappa Coefficient
HPT	Asuncion, Davao del Norte	86.14	0.69
	Enrile, Cagayan	72.28	0.5225
SMI	Ilocos Norte	72.28	0.4957
	Albay	87.13	0.8033
Average		79.46	0.6279

3.3 Demonstration of the capability of HPT for post-disaster assessment

The classification maps of Enrile, Cagayan derived from Diwata-1 and Landsat-8 after the area was hit by Super Typhoon Lawin are shown in Figure 8. The post-disaster classification map from Diwata-1 (Figure 8a) taken five days after Lawin hit the area shows flooded agricultural lands covering 1,004,667 m^2 or 33.35% of the scene. However, the classification map from Landsat-8 (Figure 8b) acquired seven days after the typhoon shows a smaller flooded area wherein only 526,500 m^2 is covered by water, about 16.83% of the scene. Just after two days, the water in those agricultural areas subsided and about half of the original flooded area has already dried up. Since Landsat-8 only revisits every after 16 days, Diwata-1 can be utilized in days where there are no Landsat pass to aid in the assessment of damage due to disasters. In addition, since the HPT sensor has a higher resolution of 3 meters, damaged areas can be assessed more accurately.

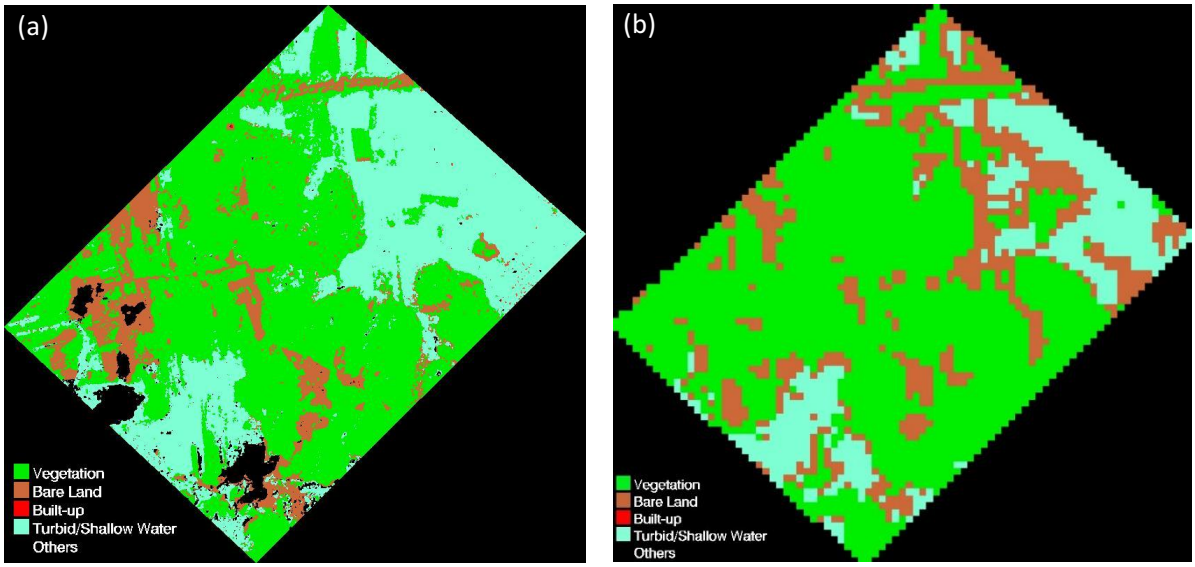

Figure 8. Land cover classification maps of Enrile, Cagayan from (a) Diwata-1 and (b) Landsat-8 after it was hit by Super Typhoon Lawin.

CONCLUSION

Using the images captured by the HPT and SMI sensors of Diwata-1, land cover and water types were successfully classified with high accuracy. From the results of the accuracy assessment, the derived classification maps have an average overall accuracy of 79.46% and a substantial average kappa coefficient of 0.6279. Based on the results, shallow water bodies were successfully delineated from the deep waters and vegetated areas were differentiated from non-vegetated ones. The inclusion of NDVI in classification of SMI images has significant impact in improving the classification of vegetation and clear water bodies. The sources in error in classification include the acquisition of some images in non-optimal time, the gap in acquisition dates of the Diwata-1 images and the reference map, similarity in spectral response of the bare and built-up classes, mixing of pixels and slight shift in georeferencing. Nonetheless, the positive result from the accuracy assessment means that the derived classification maps from Diwata-1 can be used for various applications such as post-disaster assessment, as demonstrated in this study.

REFERENCES

Al-doski, J., Mansor, S., and Shafri H., 2013. NDVI differencing and post-classification to detect vegetation changes in Halabja City, Iraq. IOSR Journal of Applied Geology and Geophysics, 1(2), pp. 1-10.

Bernstein, L., Jin X., Gregor B., and Adler-Golden S., 2012. Quick atmospheric correction code: Algorithm description and recent upgrades. Optical Engineering, 51(11), pp. 111719-1-11.

Congalton, R., 1991. A review of Assessing the Accuracy of Classifications of Remotely Sensed Data. Remote Sensing of Environment, 37, pp. 35-46.

Defries R., and Townshend J., 1994. NDVI-derived land cover classifications at a global scale. International Journal of Remote Sensing, 15(17), pp. 3567-3586.

Landis, J., and Koch G., 1977. The measurement of observer agreement for categorical data. Biometrics, 33(1) pp. 159-174.

Morawitz, D., Blewett, T., Cohen, A., and Alberti M., 2006. Using NDVI to assess vegetative land cover change in central Puget Sound. Environmental Monitoring and Assessment, 114, pp. 85-106.

Richards, J., and Jia X., 2006. Remote Sensing Digital Image Analysis. Springer, Berlin, pp. 193-200.

Rouse, J., Haas R., Schell J., and Deering D., 1974. Monitoring vegetation systems in the Great Plains with ERTS. Proceedings of the Third Earth Resources Technology Satellite -1 Symposium, 1, pp. 48-62.

Story, M., and Congalton, R., 1986. Accuracy assessment: a user's perspective. Photogrammetric Engineering and Remote Sensing, 52(3), pp. 397-399.